ISSN: 2688-8645

# Study on the Influence of Base Fluid Properties on the Performance of Carbon Dioxide Foam Fracturing Fluids

Xiaolong Wang

School of Mechanical Engineering, Xi'an Shiyou University, Xi'an, Shaanxi 710065, China

## Abstract

**$CO_2$ foam fracturing fluids, commonly used in fracturing deep unconventional oil and gas reservoirs, currently suffer from poor stability, high friction resistance, and inadequate sand-carrying capacity. This study selected three base fluids: guanidine gel (traditional system), G509 surfactant composite system, and SCF novel polymer system. Testing was conducted using a high-temperature, high-pressure foam generator and a high-temperature, high-pressure rotational rheometer system.The stability, rheology, and sand-carrying properties of carbon dioxide ($CO_2$) foam fracturing fluids were investigated under three different base fluid types. Using a high-temperature, high-pressure visual reactor, the foam stability in both liquid and supercritical states was evaluated via the half-life method. Rheological parameters were measured using a rotational rheometer, and the constitutive equation was fitted. Combined with clay aggregate settling experiments, the sand-carrying characteristics under actual operating conditions were analyzed.Experimental results indicate that under liquid $CO_2$ conditions, the SCF system exhibits optimal stability with virtually no liquid phase separation within 300 minutes. Under supercritical $CO_2$ conditions, both the guanidine-gum system and SCF system exhibited half-lives of 293 min, significantly outperforming the G509 system (14 min). Regarding rheological properties, all three systems demonstrated pseudoplastic behavior, with the SCF system maintaining superior viscosity retention under high shear conditions. In terms of sand-carrying capacity, the SCF system exhibited the longest aggregate settling time (>80 min) and the best sand-carrying performance.To provide reference for selecting fracturing fluid systems for deep unconventional oil and gas reservoirs.**

## Keywords

**Carbon Dioxide Foam Fracturing Fluid; Base Fluid System; Stability; Rheological Properties; Sand-carrying Capacity.**

## 1. Introduction

With the continuous growth in global demand for oil and gas resources and the increasing depletion of conventional reserves, unconventional oil and gas (such as shale gas and tight oil and gas) have become the core focus of exploration and development efforts [1].Deep reservoirs (buried depth > 3000 m) are characterized by high temperature, high pressure, and low porosity/permeability. Traditional hydraulic fracturing techniques suffer from issues such as significant fluid loss, severe reservoir damage, and difficult fluid recovery, which constrain the efficient development of deep reservoirs [2-3].$CO_2$ foam fracturing fluid has emerged as the preferred technology for fracturing deep unconventional oil and gas reservoirs due to its advantages of low density, low filtrate loss, biodegradability, minimal reservoir damage, and dual functions of enhancing production and displacing oil [4-5].

As the core component of $CO_2$ foam fracturing fluid, the base fluid's chemistry, molecular weight, and molecular structure directly determine the foam's stability, rheological properties,

ISSN: 2688-8645

and sand-carrying capacity [6].Currently, commonly used base fluid systems in industrial applications include guanidine-based natural polymers, surfactant composite systems, and novel synthetic polymer systems. However, these different systems exhibit significant performance variations under high-temperature and high-pressure deep reservoir conditions [7].Although guanidine-based fluids exhibit favorable thickening and foaming properties, they suffer from poor temperature and shear resistance, and their high residual content may cause reservoir blockage. Surfactant composite systems foam rapidly but lack sufficient foam stability, making them unsuitable for extended operations. While novel polymer-based fluids (e.g., SCF systems) demonstrate potential for superior performance, systematic evaluations of their properties and compatibility studies remain inadequate [8-9].

Based on this, this paper selected three typical base fluids: guanidine-based gel, G509 surfactant composite system, and SCF novel polymer system. to construct $CO_2$ foam fracturing fluid systems. Through systematic experimental testing, the foam stability, rheological properties, and pipeline flow (sand-carrying) performance of these systems were investigated and compared under both liquid and supercritical $CO_2$ phases. Combined with experimental observations, an in-depth analysis of the performance differences among the systems was conducted to provide data support and technical references for the scientific selection and performance optimization of fracturing fluid systems for deep reservoirs.

## 2. Materials and Methods

### 2.1. Materials

#### 2.1.1. Base-Solvent System

(1) Guanidine-based gel solution: Hydroxypropyl guanidine (industrial grade, purity ≥92%) is selected and formulated at a concentration of 0.5 wt%. At low temperatures, the molecular chains become tightly entangled, providing excellent thickening effects.

(2) G509 Base Fluid: A proprietary surfactant composite system developed by Sichuan Drilling, primarily composed of sodium dodecyl sulfate (industrial grade) blended at a concentration of 0.5 wt%, delivering excellent foaming properties.

(3) SCF Base Fluid: A novel polymer system independently developed by Sichuan Drilling, primarily composed of modified polyacrylamide (industrial grade). Its long-chain molecular structure provides superior shear stability compared to traditional guanidine-based polymers.

#### 2.1.2. Other Materials

The $CO_2$ gas used in the experiment had a purity of ≥99.99% and was purchased from Xi'an Standard Industrial Gas Co., Ltd., stored in liquid form. The proppant was 40/70 mesh ceramic beads.

### 2.2. Experimental Instruments

High-Temperature, High-Pressure Visualization Reactor (Chuanqing in-house production, max pressure 50 MPa, max temperature 200°C); Rotational Rheometer (Model MCR-302, shear rate range 0.01–1000 $s^{-1}$, pressure range 0–35 MPa, temperature range -20–200°C); High-speed stirrer (FS-1500 model, speed range 0-3000 rpm); Electronic balance (FA2004 model, accuracy 0.1 mg); Low-temperature cooling circulator (DLSB-5/20 model, temperature control range -20-100°C).

### 2.3. Experimental Design and Testing Methods

#### 2.3.1. Preparation of $CO_2$ Foam Fracturing Fluid

Base Solution Preparation: According to the specified concentration requirements, dissolve the three base solution raw materials separately in water using a high-speed mixer. Due to its higher viscosity, the guanidine gum base solution requires stirring at 1500 rpm for 5 minutes.

ISSN: 2688-8645

The G509 base solution and SCF base solution should be stirred at 1500 rpm for 5 minutes to ensure complete dissolution of raw materials without lumps.Foam Preparation: Inject the prepared base fluid into a high-temperature, high-pressure visual reaction vessel. After sealing, introduce $CO_2$ gas to maintain a gas-to-liquid volume ratio of 1:1. Activate the agitator (speed 1500 rpm) and stir for 10 minutes to produce a stable $CO_2$ foam fracturing fluid. Ensure the foam's initial half-life exceeds 30 minutes to prevent premature collapse during testing.

### 2.3.2. Stability Testing

Test Conditions: Two typical operating conditions were established: liquid $CO_2$ conditions (temperature 10°C, pressure 5 MPa) and supercritical $CO_2$ conditions (temperature 70°C, pressure 10 MPa). The supercritical $CO_2$ conditions were set based on actual temperature and pressure parameters of deep reservoirs. Test Method: The prepared $CO_2$ foam fracturing fluid was placed in a high-temperature, high-pressure visual reactor. A low-temperature cooling circulator or oil bath was activated and adjusted to the set temperature. The pressure was then regulated to the target value using a high-pressure pressure-reducing valve and a nitrogen gas replenishment device. Initiate the data acquisition system to record the volume of precipitated liquid, foam height, temperature, and pressure at the bottom of the reactor every 20 minutes. When the precipitated liquid volume reaches 50% of the initial base liquid volume, the elapsed time recorded represents the foam half-life. If the precipitated liquid volume does not reach 50% within 300 minutes, record the precipitated liquid volume at the 300-minute mark.

### 2.3.3. Rheological Properties Testing

Test Conditions: Consistent with stability testing conditions, namely liquid $CO_2$ conditions (10°C, 5 MPa) and supercritical $CO_2$ conditions (70°C, 10 MPa). The shear rate range is set at 0.1–1000 $s^{-1}$, covering the shear rate range during the pumping phase of fracturing operations.

Test Method: Inject the prepared $CO_2$ foam fracturing fluid into the rheometer sample cell. After sealing, adjust to the set temperature and pressure. Once the system stabilizes, start the rheometer. Gradually increase the shear rate from low to high, recording viscosity data. Within the high-shear range of 500–1000 $s^{-1}$, increase the data recording interval to one set per 100 $s^{-1}$. Based on the obtained viscosity data, derive the relationship between shear stress and shear rate ($\tau = \eta\gamma$, where $\tau$ is shear stress, $\eta$ is viscosity, and $\gamma$ is shear rate). Fit a power-law model ($\tau = K\gamma^n$, where K is the consistency coefficient and n is the flow behavior index).

### 2.3.4. Suspended Sand Performance Test

Test conditions: Observe the settling time of ceramic aggregates as the temperature rises from the liquid state (10°C, 5 MPa) to the supercritical state (70°C, 10 MPa).

Experimental Procedure: Add 100g of ceramic beads to the foam system. After thorough mixing, cease stirring and record the settling process. Simultaneously measure the height of the suspension layer within the reactor (total height 30cm).

Key Definitions: 1) Complete settling time t: The time required for all expanded clay aggregates to reach the bottom of the reactor (min); 2) Partial settling velocity vs': The ratio of the suspended layer height H' at 60 min to the settling time t (cm/min, applicable to systems not fully settled); 3) Complete settling velocity vs: The ratio of the total height 30 cm to the complete settling time t (cm/min).

ISSN: 2688-8645

# 3. Results and Discussion

## 3.1. Experimental Study on Stability Characteristics

### 3.1.1. Precipitation of Different Base Liquids under Liquid Conditions

Under liquid conditions, all three base liquid systems exhibit satisfactory foaming performance. Among them, the SCF system demonstrates the highest foaming ratio, followed by the G509 system, while the guanidine-based system yields the lowest foaming ratio. Foams generated by all three systems exhibited a dense, uniform texture where individual bubbles were indistinguishable to the naked eye, indicating that the foaming properties of the base liquids were effectively harnessed under liquid $CO_2$ conditions. In terms of stability, the SCF system demonstrated the best performance, with liquid separation volume remaining below 20 mL within 300 minutes—significantly lower than the guanidine gel system (48 mL) and the G509 system (300 mL). The G509 system exhibited the shortest half-life (57 min). Although it demonstrated good initial foaming performance, its foam liquid membrane strength was low, leading to rapid liquid separation and growth due to easy rupture in the later stages. The guanidine system, despite having a half-life exceeding 300 min, released 48 mL of liquid within 300 min, indicating weaker actual stability compared to the SCF system.Analysis of the causes reveals that the modified polyacrylamide long-chain molecules in the SCF system can form a dense adsorption film on the surface of the bubble liquid membrane, effectively inhibiting bubble coalescence and liquid membrane drainage, thereby enhancing foam stability. Although the guanidine system can thicken the liquid membrane through molecular entanglement, its low-temperature stability is limited. After prolonged storage, molecular chains tend to disentangle, leading to a decrease in liquid membrane strength. The G509 system relies on surfactants to reduce surface tension for foaming, but lacks a long-lasting, stable liquid film support structure, resulting in the poorest stability.

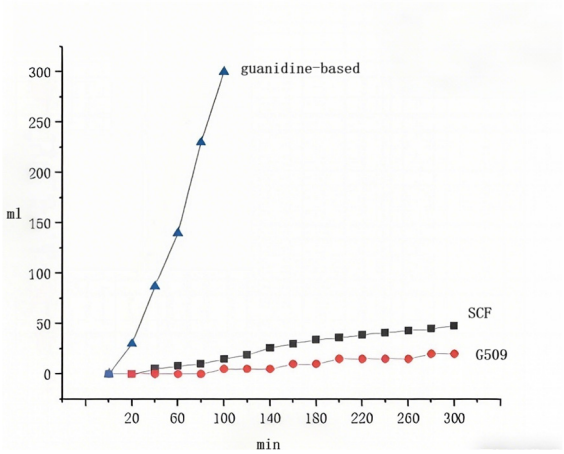


**Figure 1.** Precipitation conditions of different liquid systems

### 3.1.2. Precipitation of Different Base Liquids under Supercritical Conditions

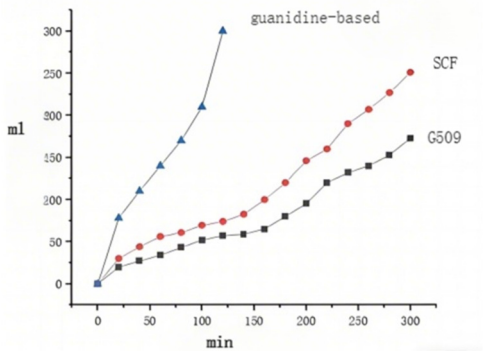


**Figure 2.** Precipitation conditions of different systems in the supercritical state

ISSN: 2688-8645

Under supercritical $CO_2$ conditions, the foaming ratio and stability of the three base liquid systems both decreased compared to liquid conditions. This is attributed to the density and viscosity of supercritical $CO_2$ lying between those of gas and liquid phases, which weakens its support for the foam liquid film. Additionally, the high-temperature, high-pressure environment accelerates liquid drainage from the film and bubble coalescence [10].The volume-time curve of precipitated liquid in Figure 2 clearly shows that the G509 system exhibits the fastest increase in precipitated liquid volume, reaching its half-life in just 14 minutes with the steepest slope. This indicates extremely poor stability under supercritical conditions. The guanidine gel system and SCF system exhibit similar slopes in their precipitate volume growth curves, both with a half-life of 293 minutes. However, the guanidine gel system shows a lower precipitate volume within the same timeframe.

### 3.1.3. Comparison of Experimental Results

Test results under both liquid and supercritical $CO_2$ conditions reveal: 1) The G509 system exhibits the poorest stability under all operating conditions, with a half-life of only 57 minutes in liquid conditions and a mere 14 minutes in supercritical conditions, rendering it unsuitable for long-term fracturing operations in deep reservoirs. 2) In liquid conditions, the SCF system demonstrates optimal stability with negligible precipitation within 300 minutes, followed by the guanidine gel system. 3) Under supercritical conditions, the guanidine gel system and SCF system share identical half-lives (293 min), but the guanidine gel system exhibits lower precipitate volume and superior stability; 4) Overall, all three systems demonstrate better stability in liquid $CO_2$ than in supercritical conditions, closely related to the physical properties of supercritical $CO_2$ and the destructive effects of high temperature and pressure on liquid film structures.

## 3.2. Rheological Characterization Experiments

### 3.2.1. Comparison of Viscosity Properties under Supercritical Conditions

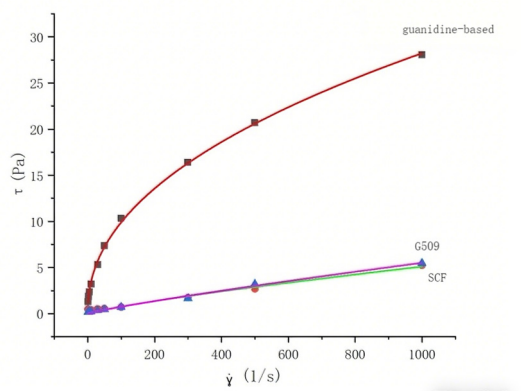


**Figure 3.** Liquid power-law fitting curve

**Table 1.** Supercritical power-law fit value

| system | Formula | k | n |
|---|---|---|---|
| Supercritical Guar gum | $\tau=K\gamma^n$ | 1.261 | 0.450 |
| Supercritical SCF | $\tau=K\gamma^n$ | 0.022 | 0.788 |
| supercriticalG509 | $\tau=K\gamma^n$ | 0.011 | 0.9904 |

ISSN: 2688-8645

Under supercritical $CO_2$ conditions, all three base-fluid $CO_2$ foam fracturing fluids exhibit pseudoplastic behavior (flow behavior index n < 1). Their viscosity decreases with increasing shear rate, demonstrating a pronounced shear thinning effect. This characteristic aligns with fracturing fluid operational requirements: high viscosity at low shear rates to ensure sand-carrying capacity, and reduced viscosity at high shear rates to minimize pumping friction losses [11].In terms of viscosity values, at low shear rates (10 $s^{-1}$), the guanidine-based system exhibited the highest viscosity (1319 mPa·s), followed by the SCF system (548.8 mPa·s), while the G509 system showed the lowest viscosity (353.6 mPa·s). At high shear rates (1000 $s^{-1}$), the viscosities of all three systems decreased significantly: the SCF system reached 5.7 mPa·s, the G509 system reached 4.87 mPa·s, and the guanidine-based system reached 28 mPa·s. Regarding the degree of viscosity reduction, the SCF system exhibited the greatest decrease (98.9%), followed by the G509 system (98.6%), while the guanidine-based system showed the smallest reduction (97.9%). This indicates that the SCF system demonstrates a more pronounced shear thinning effect and is better suited for the high-shear conditions encountered during pump injection processes.

As shown by the power-law fitting curves in Figure 4, the rheological data of all three systems exhibit high conformity with the power-law model, indicating that this model effectively describes their rheological characteristics [12]. The guanidine hydroxide system exhibits the highest viscosity coefficient K (1.26 Pa·s^n), indicating its strongest thickening capacity. However, its flow behavior index n is the smallest (0.45), signifying the most pronounced pseudoplastic behavior. Under high shear, its viscosity decreases relatively little, potentially leading to increased pumping friction resistance. The SCF system exhibits intermediate K and n values, balancing good thickening capacity with shear thinning effects. The G509 system has the lowest K value (0.01 Pa·$s^n$), indicating the weakest thickening ability. Its n value is closest to 1 (0.90), suggesting relatively weak shear thinning effects. Its insufficient viscosity under low shear conditions may fail to meet sand-carrying requirements.

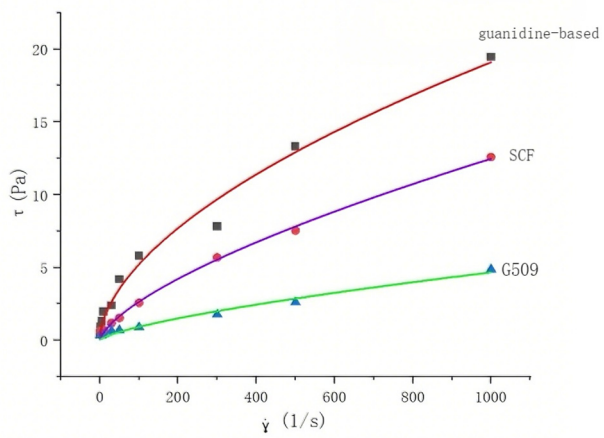


**Figure 4.** Supercritical power-law fitting curve

**Table 2.** Liquid power-law fitting value

| system | Formula | k | n |
|---|---|---|---|
| Liquid Guar gum | $\tau=K\gamma^n$ | 0.479 | 0.538 |
| Liquid SCF | $\tau=K\gamma^n$ | 0.124 | 0.668 |
| Liquid G509 | $\tau=K\gamma^n$ | 0.044 | 0.679 |

ISSN: 2688-8645

Under liquid $CO_2$ conditions, all three base liquid systems exhibit pseudoplastic behavior with pronounced shear thinning effects [13].Compared to supercritical conditions, the viscosity of all three systems significantly increases under liquid conditions. This is attributed to the higher density of liquid $CO_2$, which provides stronger support to the foam liquid film, while the low-temperature environment inhibits degradation of the base liquid molecular chains, resulting in higher liquid film viscosity [14]. At low shear rates (10 $s^{-1}$), the guanidine hydroxide system exhibited the highest viscosity (2150 mPa·s), followed by the SCF system (1860 mPa·s), while the G509 system showed the lowest viscosity (1280 mPa·s). At high shear rates (1000 $s^{-1}$), the viscosity ranking remained consistent: guanidine gel system at 42 mPa·s, SCF system at 38 mPa·s, and G509 system at 32 mPa·s. Regarding viscosity reduction, the three systems showed minimal variation, ranging between 97.5% and 98.0%.

Based on the power-law fitting results, the guanidine-based system and SCF system exhibit higher fitting accuracy, while the G509 system shows relatively lower fitting accuracy. This indicates that the rheological properties of the G509 system are more complex under liquid conditions. The flow behavior index n (0.42) of the SCF system is greater than that of the guanidine hydrochloride system (0.38), indicating weaker pseudoplasticity characteristics. This results in a more gradual viscosity change during pumping, which is more conducive to stable sand transport. The G509 system has the highest n value (0.68) and the weakest pseudoplasticity characteristics, making the issue of insufficient viscosity under low shear stress more pronounced [15].

## 3.3. Study on the Sand-Carrying Performance of Guanine Gum

If sand-carrying capacity is insufficient, proppants may prematurely settle and accumulate near the wellbore in the fracture zone, resulting in unfilled fractures at the distal end and reduced flow capacity. Simultaneously, settled proppants may clog the wellbore, complicating backflow operations [16-19]. By investigating the sand-carrying mechanism of $CO_2$ foam fracturing fluids, the influence patterns of factors such as gas-liquid ratio, foam stabilizer type, and shear rate on sand-carrying capacity can be clarified. This enables the optimization of fracturing fluid systems characterized by “high sand-carrying capacity and low formation damage” [20-23].

### 3.3.1. Study on Sand-Carrying Performance of Clay Aggregates

Experimental conditions under liquid conditions: 300 mL guanidine-based liquid, 300 mL liquid $CO_2$, 300 mL liquid $CO_2$ added at 10°C under 4.32 MPa pressure. Simultaneously add 100 g of ceramic aggregates while initiating stirring. After achieving complete homogeneity, proceed with temperature elevation. At 70°C, record precipitation data and phenomena every 10 minutes.

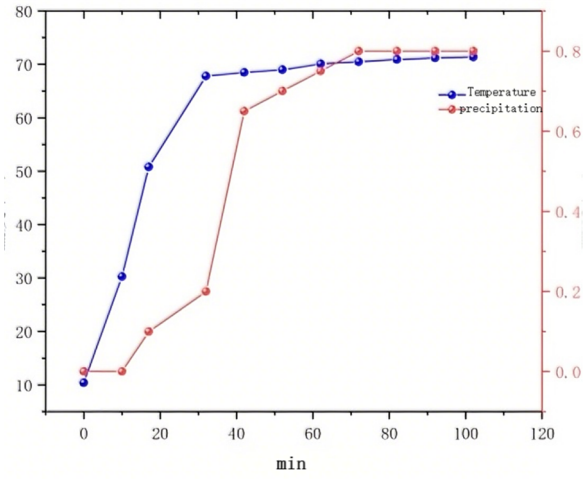


**Figure 5.** Changes in guanidinium gel gravel sedimentation

ISSN: 2688-8645

During the heating process from 10°C to 70°C, ceramic particles began to separate from the foam surface at 30°C. At the critical temperature of 67.8°C, a large number of ceramic particles adhered to the foam surface, accompanied by particle deposition.

After 70°C, as time progresses, the ceramic particles adhering to the foam surface begin to settle. By 60 minutes, the particles have largely settled completely, with liquid separation occurring. A distinct layering phenomenon becomes evident at 70 minutes.

### 3.3.2. Study on Sand-Carrying Performance of SCF System

Experimental conditions under liquid conditions: 300 mL SCF base liquid, 300 mL liquid $CO_2$, 300 mL liquid $CO_2$ added at 10°C under 4.7 MPa pressure. Simultaneously add 100 g ceramic particles while initiating stirring. After achieving complete homogeneity, proceed with temperature elevation. At 70°C, record precipitation data and phenomena every 10 minutes.

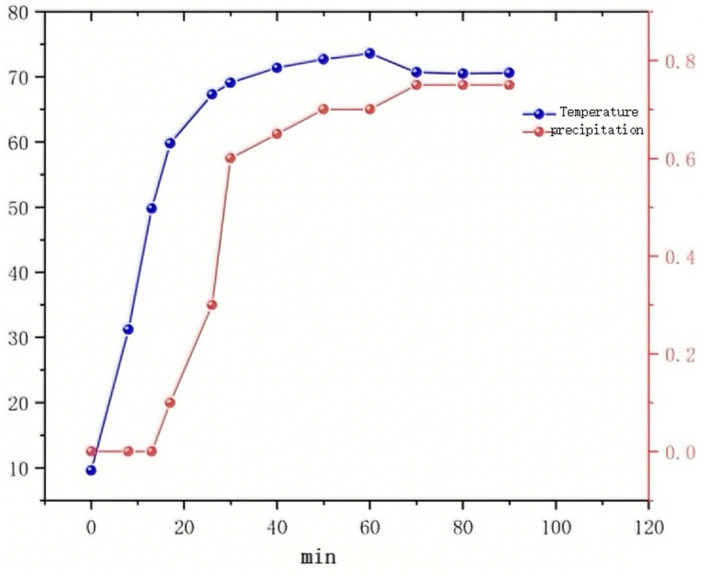


**Figure 6.** SCF Gravel Settlement Changes

Temperature increased from 10°C to 70°C. During heating, ceramic particles began to separate from the foam surface at 30°C. At the critical temperature of 67.8°C, ceramic particles adhered to the foam surface, accompanied by minor particle deposition.

After 70°C, the ceramic particles entered a settling state. Over time, the particles adhering to the foam surface began to settle. After 80 minutes, the particles had not fully settled, no liquid had separated out, and a significant amount of ceramic particles remained suspended on the foam surface.

### 3.3.3. Study on Sand-Carrying Performance of G509

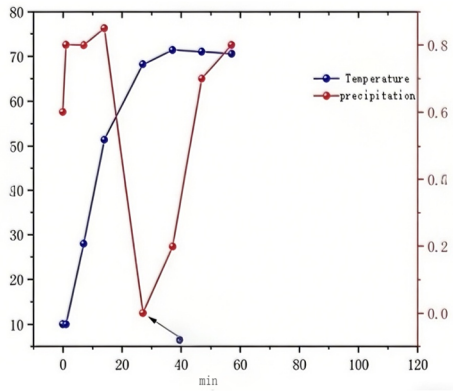


**Figure 7.** G509 Gravel Settlement Changes

ISSN: 2688-8645

Experimental conditions under liquid conditions: 300 mL of G509 base liquid, 300 mL of liquid $CO_2$, with 300 mL of liquid $CO_2$ added at 10°C under a pressure of 4.64 MPa. While initiating stirring, 100 g of ceramic aggregate was added. After achieving complete and uniform mixing, the mixture underwent a temperature increase treatment. At 70°C, precipitation data and phenomena were recorded every 10 minutes.

Temperature increased from 10°C to 70°C. During the heating process, the ceramic granules had largely settled within 1 minute, and were fully settled at 28°C.

As shown in Figure 9, the ceramic particles had fully settled by 68°C. After re-mixing the foam and ceramic particles, the settling state was recorded once thoroughly blended. Significant sedimentation occurred at 10 minutes, with complete settling and noticeable liquid separation at 20 minutes, accompanied by distinct stratification. Substantial liquid separation was observed at 30 minutes.

### 3.4. Comprehensive Performance Comparison and Discussion

Based on all performance metrics, the SCF novel polymer-based fluid demonstrated the most outstanding comprehensive performance: it maintained excellent foam stability and good rheological shear thinning properties in both phases, while its superior sand-carrying capacity ensured effective delivery and placement of proppants within fractures. The guanidine polymer system exhibits stability comparable to SCF under supercritical conditions and features high low-shear viscosity. However, its temperature and shear resistance are relatively weak, and it carries potential reservoir damage risks. The G509 surfactant system, despite its good foaming performance, suffers from severely inadequate foam stability (especially at high temperatures) and sand-carrying capacity, making it difficult to meet the requirements for long-term, efficient fracturing operations in deep reservoirs.

## 4. Conclusion and Outlook

(1) Stability: Under liquid $CO_2$ conditions, the SCF system exhibited optimal stability with negligible precipitation within 300 min and a half-life exceeding 300 min. Under supercritical conditions, both the SCF and guanidine gel systems showed a half-life of 293 min, but the SCF system demonstrated superior stability with less liquid precipitation. The G509 system performed worst in both liquid and supercritical conditions, failing to meet construction requirements.

(2) In terms of rheological properties: All three systems exhibit pseudoplastic behavior with shear thinning effects. Under liquid conditions, the guanidine-glucofuranose system demonstrates the highest viscosity, while the SCF system offers a favorable balance between viscosity and shear thinning. Under supercritical conditions, the SCF system exhibits the most pronounced shear thinning effect, making it suitable for high-shear pumping applications. Power-law models achieve a goodness-of-fit exceeding 0.99, indicating stable rheological characteristics.

(3) Sand-carrying capacity: The SCF system exhibits the longest complete settling time for ceramic aggregates (>80 min), with significantly superior sand suspension capability compared to the guanidine-based system (60 min) and the G509 system (30 min).

(4) Comprehensive Performance Evaluation: The SCF novel polymer-based liquid $CO_2$ foam fracturing fluid demonstrates optimal integrated performance in foam stability, rheological properties, and sand-carrying capacity, making it the preferred system for fracturing and modification of deep, high-temperature, high-pressure unconventional oil and gas reservoirs.

Future research may focus on the following areas: 1) Further optimizing the molecular structure and formulation of SCF base fluids to enhance their performance under extreme conditions of higher temperatures (>150°C) and pressures (>30 MPa); 2) Conducting large-

scale indoor simulation circulation tests and field pilot trials based on specific onsite parameters such as flow rate and pipe diameter to validate and optimize the practical application effectiveness of this system [24]; 3) Deepen the investigation of the structure-property relationship between the polymer chain structure and interfacial properties of the base fluid and the macro-performance of the foam, providing theoretical guidance for the molecular design of a new generation of high-performance, low-damage fracturing fluid systems [25].

## References

[1] Li Gensheng, Huang Zhongwei, Niu Jilei. Advances and Prospects in Fracturing Technology for Unconventional Oil and Gas Reservoirs [J]. Acta Petrolei Sinica, 2020, 41(1): 1-21.

[2] Wang Zenglin, Zhang Shicheng, Yang Haibin. Research and Application of $CO_2$ Foam Fracturing Fluid Technology [J]. Petroleum Drilling and Production Technology, 2019, 41(3): 321-327.

[3] An Hao. Performance Testing of $CO_2$ Foam Fracturing Fluid [J]. Inner Mongolia Petrochemical Industry, 2014, 40(22): 32-33.

[4] Zhao Jinzhou, Zou Caineng, Hu Yongle. Current Status and Development Trends of Fracturing Technology in Shale Gas Development [J]. Natural Gas Industry, 2017, 37(5): 1-10.

[5] Liu Yijiang, Chen Mian, Jin Yan. Key Issues and Research Progress in Supercritical $CO_2$ Fracturing Technology [J]. Petroleum Exploration and Development, 2016, 43(4): 623-631.

[6] Sun Huanquan, Wang Jun, Zhang Kai. Analysis of Factors Affecting the Stability of Foam Fracturing Fluids [J]. Acta Petrolei Sinica (Petroleum Processing), 2015, 31(2): 367-373.

[7] Zhou Fujian, Yang Yongfei, Wang Xiujuan. Research and Development of Novel Polymer Foam Fracturing Fluids and Their Performance Evaluation [J]. Drilling Fluids and Completion Fluids, 2014, 31(4): 65-69.

[8] Wu Xiaolin, Li Chuanliang, Du Zhimin. Handbook of Unconventional Oil and Gas Development Technologies [M]. Beijing: Petroleum Industry Press, 2021.

[9] Ma Xinhua, Guo Tonglou, Jia Ailin. Shale Gas Reservoir Modification Technology and Practice [M]. Beijing: Science Press, 2020.

[10] Li Mingzhong, Zhang Ningsheng, Wu Xinmin. Interaction Mechanism Between Supercritical $CO_2$ and Foam Fracturing Fluid [J]. Acta Chimica Sinica, 2019, 70(8): 3056-3064.

[11] Jiang Guancheng, Wang Guijiang, Zhang Jie. Testing and Evaluation Methods for Rheological Properties of Fracturing Fluids [J]. Acta Petrolei Sinica, 2018, 39(7): 827-835.

[12] Ahmed S ,Elraies K ,Hashmet M , et al.Empirical Modeling of the Viscosity of Supercritical Carbon Dioxide Foam Fracturing Fluid under Different Downhole Conditions[J]. Energies, 2018, 11(4): 782. DOI:10.3390/en11040782.

[13] Energy; New Findings from Petronas in the Area of Energy Reported (Empirical Modeling of the Viscosity of Supercritical Carbon Dioxide Foam Fracturing Fluid under Different Downhole Conditions)[J].Chemicals & Chemistry,2018,2266-.

[14] Energy; New Findings from University of Technology in the Area of Energy Described (Empirical Modeling of the Viscosity of Supercritical Carbon Dioxide Foam Fracturing Fluid Under Different Downhole Conditions)[J].Energy & Ecology,2019,

[15] Song L ,Yu F ,Tingting H , et al.Research and performance optimization of carbon dioxide foam fracturing fluid suitable for shale reservoir[J].Frontiers in Energy Research, 2023, 11DOI: 10.3389/FENRG.2023.1217467.

[16] Jin Cheng. Preparation and Mechanism Study of Drag-Reducing Thickener with Excellent Shear Resistance and Sand-Carrying Properties [C]//Xi'an Petroleum University, China University of Petroleum (Beijing), Shaanxi Petroleum Society. Proceedings of the 2025 International Conference on Exploration and Development of Oil and Gas Fields (IFEDC). Southwest Petroleum University; 2025: 1285-1287. DOI: 10.26914/c.cnkihy.2025.071174.

ISSN: 2688-8645

[17] Huang Tao, Zhong Ying, Mou Qiuhang, et al. Technology and Sand Suspension Performance of Carbon Dioxide-Suspended Proppants in Complex Fracturing Networks [J]. Oilfield Chemistry, 2025, 42(01): 38-43+51. DOI: 10.19346/j.cnki.1000-4092.2025.01.006.

[18] Qiao, Yuzhong. Study on Drag Reduction and Sand Carrying Performance of Hydrophobic Associative Polymer Solutions [D]. Southwest Petroleum University, 2023. DOI: 10.27420/ d.cnki. gxsyc. 2023.001471.

[19] Maieryemgul Anwar, Pu Di, Zhai Huajian, et al. Development and Application of Suspension-Based High-Efficiency Drag Reduction Sand-Carrying Fracturing Fluid [J]. Oilfield Chemistry, 2022, 39(03): 387-392+400. DOI:10.19346/j.cnki.1000-4092. 2022.03.002.

[20] Shi, D.S. Study on Sand Carrying Mechanism of Liquid CO2/N2 Foam Fracturing Fluid System [D]. China University of Petroleum (East China), 2019. DOI:10.27644/d.cnki.gsydu.2019.001948.

[21] Chen, Yanqiu. Study on Flow Characteristics of Supercritical Carbon Dioxide Fracturing Fluid and Sand Transport Mechanisms in Wellbores [D]. Northeast Petroleum University, 2018.

[22] Wang Liwei, Lu Yongjun, Qiu Xiaohui, et al. Research on Sand-Carrying and Drag-Reducing Dual-Function Fracturing Fluid System and Its Rheological Properties [C]//Chinese Chemical Society, Chinese Society of Theoretical and Applied Mechanics, Rheology Professional Committee. Proceedings of the 13th National Rheology Conference. Langfang Branch, China National Petroleum Exploration and Development Research Institute; Key Laboratory of Reservoir Modification, China National Petroleum Corporation; 2016:199-204.

[23] Song Yuanfei, Sun Pengbo. Research Status and Prospects of Liquid Carbon Dioxide Fracturing Technology [J]. Science and Innovation, 2016, (19): 14. DOI: 10.15913/j.cnki.kjycx.2016.19.014.

[24] Hou Lei, Sun Baojiang, Jiang Tingxue, et al. Calculation of Proppant Trailing Behavior in Supercritical Carbon Dioxide [J]. Acta Petrolei Sinica, 2016, 37(08): 1061-1068.

[25] Wang Peng, Wang Fengshan, Zhang Qian. Analysis of Flow Pressure Drop and Sensitivity Factors in Fracturing Fluids [J]. Journal of Yangtze University (Natural Science Edition), 2016, 13(11): 60-64+5-6. DOI:10.16772/j.cnki.1673-1409.2016.11.013.